A Multifunctional Heterogeneous Catalyst: Titanium-containing Mesoporous Silica Material Encapsulating Magnetic Iron Oxide Nanoparticles

Kohsuke Mori,[1] Yuichi Kondo,[1] Shotaro Morimoto,[2] and Hiromi Yamashita*[1]
[1]*Division of Materials and Manufacturing Science, Graduate School of Engineering, Osaka University, 2-1 Yamada-oka, Suita, Osaka 565-0871*
[2]*Facility of Pharmaceutical Science, Osaka Ohtani University, 3-11-1 Nishikiori-Kita, Tondabayashi, Osaka 584-8540*

(Received May 30, 2007; CL-070583; E-mail: yamashita@mat.eng.osaka-u.ac.jp)

Magnetic iron oxide nanoparticles coated with mesoporous silica involving single-site titanium oxide moiety have been first developed by adopting a two-step coating method. The catalytic performance and magnetically separable ability were demonstrated in the oxidation of 2,6-di-*tert*-butylphenol using hydrogen peroxide.

The development of prominent heterogeneous catalysts with well-defined surface structure that enable rapid and selective chemical transformations and can be separated completely from the product is a paramount challenge.[1] Among several catalyst materials, mesoporous molecular sieves featuring large surface area as well as ordered hexagonal mesopore channels ranging from 2–10 nm are classified as promising catalyst supports.[2] These materials have often been doped with heteroatoms, e.g., Ti, Cr, Mo, etc., generating potentially active site that exhibits the requisite activity and selectivity for specific catalytic reactions.[3] The transition-metal oxide moieties are considered to be highly dispersed at the atomic level and also to be well-defined catalysts, which exist in the specific structure of the framework. However, the difficulties in recovering the small mesoporous silica particles from the reaction mixture severely circumvent their industrial applications. In order to overcome the above drawbacks, the fabrication of mesoporous silica incorporating magnetic nanoparticles would be a promising strategy: it is possible to recover the composite materials from the liquid system using external magnet. Although the synthesis of magnetic mesoporous silica by grafting or encapsulating magnetic nanoparticles have been reported recently, the coating material is limited to pure silica so far.[4]

Herein, we first developed Ti-containing hexagonal mesoporous silica (Ti-HMS) encapsulating magnetic iron oxide nanoparticles (Fe_xO_y@Ti-HMS). The designed architecture enables the powerful combination of useful functions, superparamagnetism, catalytically active site, and mesoporous structure.

We adopted the two-step coating method as a synthetic strategy. Thus, a silica layer was first deposited on the surface of iron oxide nanoparticles in order to protect and facilitate the formation of Ti-HMS phase. Then, the Ti-HMS layer was formed from subsequent sol–gel polymerization of tetraethylorthosilicate (TEOS), tetrapropylorthotitanate (TPOT), and dodecyamine. The synthetic procedure is as follows. Initially, a mixture of the ferrous and ferric salt solutions ($Fe^{2+}/Fe^{3+} = 0.5$) was introduced into an NH_4OH solution. To the resulting black nanoparticles solution, TEOS was added dropwise with mechanical stirring. The resultant black powder was calcined at 523 K for 2 h to give the silica-coated iron oxide (Fe_xO_y@SiO_2) as a reddish-brown powder. This color change is originated from the transformation of Fe_3O_4 phase into γ-Fe_2O_3. It is well known that the coprecipitation of ferrous and ferric ions in a basic aqueous solution first gives Fe_3O_4 nanoparticles, which can be directly oxidized into γ-Fe_2O_3 by aeration.[5] Next, a source of Ti-HMS (TEOS, TPOT, and dodecylamine) was added to the Fe_xO_y@SiO_2 dispersed in 2-propanol, followed by calcination at 823 K for 5 h, giving Fe_xO_y@Ti-HMS (Si: 42.0, Fe: 7.4, Ti: 0.64 wt %).

In the low-angle XRD pattern, the Fe_xO_y@Ti-HMS exhibits a diffraction peak at around $2\theta = 3^\circ$ associated with the d_{100} spacing, indicating the presence of hexagonally packed mesoporous structure (Figure 1A). The wide-angle XRD pattern shows clear peaks due to either Fe_3O_4 or γ-Fe_2O_3 phase or both at around 30.3, 35.6, 43.7, 54.1, 57.5, and 63.2°, corresponding to the (220), (311), (400), (422), (511), and (440) reflections, respectively (Figure 1B). Distinguishing between Fe_3O_4 and γ-Fe_2O_3 phase by XRD is quite difficult because of the same inverse spinel structure and similarity in their d spacing. The Raman spectrum, which is often applied as a useful technique for differentiating various iron oxide phases, showed a characteristic band of γ-Fe_2O_3 phase at around 1400 cm^{-1} (Figure 1S).[11]

N_2 adsorption–desorption showed the typical type IV isotherm without significant hysteresis loop (Figure 2S).[11] The BET surface area was found to be 910 $m^2 \cdot g^{-1}$. The pore size distribution calculated from desorption of the N_2 isotherm by the BJH method showed that an average pore size of 3.0 nm with narrow size distributions.

TEM image showed the formation of the iron oxide nanoparticles having size between 5 and 13 nm, and the average diameter of ca. 9.5 nm were found to be distributed within the host silica matrix (standard deviation: $\sigma = 0.2$ nm, $\sigma/d = 21.7\%$) (Figure 3S).[11]

The isothermal magnetization curve of the Fe_xO_y@Ti-HMS at 300 K displayed a rapid increase with increasing applied mag-

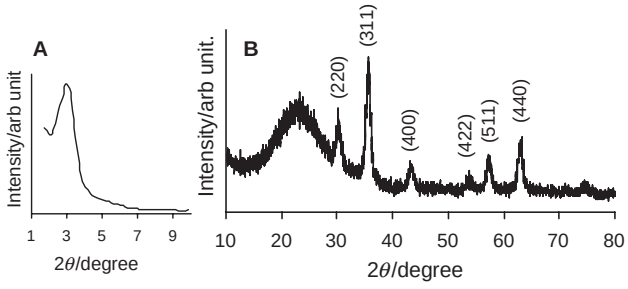

Figure 1. (A) Low-angle and (B) wide-angle XRD patterns of Fe_xO_y@Ti-HMS.

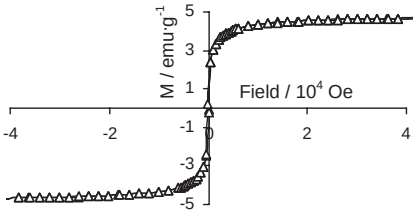

Figure 2. Field-dependent magnetization curve for Fe_xO_y@Ti-HMS measured at 300 K.

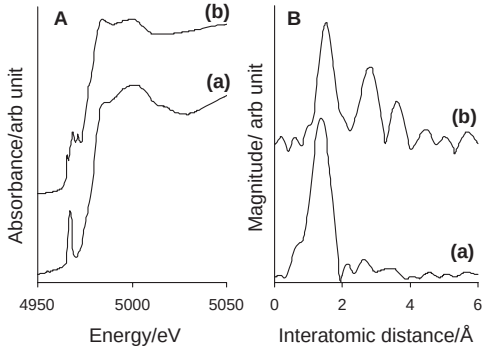

Figure 3. (**A**) Ti K-edge XANES spectra and (**B**) FT-EXAFS spectra for (a) Fe_xO_y@Ti-HMS and (b) TiO_2 powder (P25).

netic field due to superparamagnetic relaxation (Figure 2).[6] Hysteresis was absent with zero remanence and coercivity, and the saturation magnetization (M_s) reached up to 4.65 emu/g. When normalized to the γ-Fe_2O_3 content in the sample, the M_s of 65 emu/g for γ-Fe_2O_3 in the Ti-HMS matrix is smaller than the theoretical value of 76 emu/g for bulk γ-Fe_2O_3 at room temperature.[7] This difference can be explained by the defined size effects responsible for the degradation of magnetic properties in iron oxide nanoparticles.

Figure 3A shows the Ti K-edge XANES spectra of the Fe_xO_y@Ti-HMS and TiO_2 powder (P25: anatase 80%, rutile 20%). TiO_2 powder gives rise to several well-defined preedge peaks attributable to the titanium in a symmetric octahedral environment. On the contrary, the Fe_xO_y@Ti-HMS exhibits an intense single preedge peak at 4967 eV corresponding to a dipolar-allowed transition from the 1s to t_2 molecular levels built from the 3d and 4p metal orbital and from a neighboring orbital.[8] The observation of this intense single preedge peak indicates that the titanium oxide moieties have a tetrahedral coordination. In the FT-EXAFS data (Figure 3B), the peak suggestive of contiguous Ti–O–Ti bond was observed in the TiO_2 powder. On the contrary, the Fe_xO_y@Ti-HMS showed only a strong peak at around 1.6 Å assignable to the neighboring oxygen atoms due to a Ti–O bond.

The potential catalytic ability of the Fe_xO_y@Ti-HMS was investigated in the oxidation of a sterically bulky 2,6-di-*tert*-butyl phenol (2,6-DTBP) using 30% hydrogen peroxide (H_2O_2). The corresponding quinone was obtained in 97% yield with 99% selectivity (Table 1). In comparison, the oxidation using anatase TiO_2 hardly occurred because of the undesired decomposition of H_2O_2 by contiguous Ti–O–Ti bonds.[9] It has been reported that the large 2,6-DTBP can not diffuse into the small micropore of TS-1 and, therefore, can not be transformed.[10] These comparisons of oxidation results confirm the formation of isolated and tetrahedral titanium oxide moiety located on the mesoporous framework, as shown by the Ti K-edge XAFS analysis.

Table 1. Oxidaton of 2,6-DTBP using Fe_xO_y@Ti-HMS catalyst and recycling results

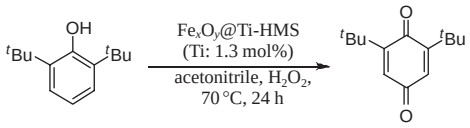

Run	1st	2nd	3rd	4th	5th
Initial rate /mmol·h^{-1}	0.052	0.051	0.051	0.051	0.051
Yield/%	97	97	97	97	97
Select./%	>99	>99	>99	>99	>99

Upon completion of the oxidation reaction, the magnetic properties of the Fe_xO_y@Ti-HMS can afford a straightforward way of isolating the catalyst. By applying a permanent magnet externally, the catalyst was attracted within a few minutes. The recovered catalyst could be recycled without significant loss of its inherent activity, giving the corresponding quinine in >97% yields (TON: >74) at least four times.

In summary, a new multifunctional nanocomposite, Fe_xO_y@Ti-HMS, involving superparamagnetic iron oxide nanoparticles, ordered mesoporous channels, and isolated and tetrahedral titanium oxide moiety has been developed. The Fe_xO_y@Ti-HMS acted as an efficient heterogeneous catalyst for the liquid-phase selective oxidation reaction using H_2O_2, and its high recyclability was also demonstrated.

References and Notes

1 R. J. Wijngaarden, A. Kronberg, K. R. Westerterp, in *Industrial Catalysis: Optimizing Catalysts and Processes*, Wiley-VCH, Weinheim, **1998**.
2 Y. Tao, H. Kanoh, L. Abrams, K. Kaneko, *Chem. Rev.* **2006**, *106*, 896.
3 a) H. Yamashita, K. Mori, *Chem. Lett.* **2007**, *36*, 348. b) Y. Shiraishi, N. Saito, T. Hirai, *J. Am. Chem. Soc.* **2005**, *127*, 8304.
4 a) M. Fröba, R. Köhn, G. Bouffaud, O. Richard, G. van Tendeloo, *Chem. Mater.* **1999**, *11*, 2858. b) A.-H. Lu, W. Schmidt, N. Matoussevitch, H. Bönneman, B. Spliethoff, B. Tesche, E. Bill, W. Kiefer, F. Schüth, *Angew. Chem., Int. Ed.* **2004**, *43*, 4303. c) W. Zhao, J. Gu, L. Zhang, H. Chen, J. Shi, *J. Am. Chem. Soc.* **2005**, *127*, 8916.
5 Y. S. Kang, S. Risbud, J. F. Rabolt, P. Stroeve, *Chem. Mater.* **1996**, *8*, 2209.
6 J. M. D. Coey, D. Khalafalla, *Phys. Status. Solidi. A* **1972**, *11*, 229.
7 B. D. Cullity, in *Introduction to Magnetic Materials*, Addison-Wesley, Reading, MA, **1972**.
8 H. Yamashita, Y. Ichihashi, M. Anpo, M. Hashimoto, C. Louis, M. Che, *J. Phys. Chem.* **1996**, *100*, 16041.
9 B. Notari, *Stud. Surf. Sci. Catal.* **1998**, *37*, 413.
10 W. Zhang, M. Fröba, J. Wang, P. T. Tanev, J. Wong, T. J. Pinnavaia, *J. Am. Chem. Soc.* **1996**, *118*, 9164.
11 Supporting Information is available electronically on the CSJ-Journal Web site, http://www.csj.jp/journals/chem-lett/index.html.

Published on the web (Advance View) July 21, 2007; doi:10.1246/cl.2007.1068